Acta Pharm. **74** (2024) 37–59
https://doi.org/10.2478/acph-2024-0008

Original research paper

Novel (±)-*trans*-*β*-lactam ureas: Synthesis, *in silico* and *in vitro* biological profiling

MLADENKA JURIN[1]
VIŠNJA STEPANIĆ[2]
KRUNOSLAV BOJANIĆ[3]
DENIS VADLJA[3]
DARKO KONTREC[1]
TONKO DRAŽIĆ[4]
MARIN ROJE[1,*]

[1] *Division of Organic Chemistry and Biochemistry, Laboratory for Chiral Technologies, Ruđer Bošković Institute 10000 Zagreb, Croatia*

[2] *Division of Electronics, Laboratory for Machine Learning and Knowledge Representation, Ruđer Bošković Institute, 10000 Zagreb, Croatia*

[3] *Division of Materials Chemistry Laboratory for Aquaculture in Biotechnology, Ruđer Bošković Institute 10000 Zagreb, Croatia*

[4] *Division of Physical Chemistry Laboratory for Biocolloids and Surface Chemistry, Ruđer Bošković Institute 10000 Zagreb*

Accepted January 13, 2024
Published online January 14, 2024

ABSTRACT

A diastereomeric mixture of racemic 3-phthalimido-*β*-lactam **2a**/**2b** was synthesized by the Staudinger reaction of carboxylic acid activated with 2-chloro-1-methylpyridinium iodide and imine **1**. The amino group at the C3 position of the *β*-lactam ring was used for further structural upgrade. *trans*-*β*-lactam ureas **4a–t** were prepared by the condensation reaction of the amino group of *β*-lactam ring with various aromatic and aliphatic isocyanates. Antimicrobial activity of compounds **4a–t** was evaluated *in vitro* and neither antibacterial nor antifungal activity were observed. Several of the newly synthesized *trans*-*β*-lactam ureas **4a–c**, **4f**, **4h**, **4n**, **4o**, **4p**, and **4s** were evaluated for *in vitro* antiproliferative activity against liver hepatocellular carcinoma (HepG2), ovarian carcinoma (A2780), breast adenocarcinoma (MCF7) and untransformed human fibroblasts (HFF1). The *β*-lactam urea **4o** showed the most potent antiproliferative activity against the ovarian carcinoma (A2780) cell line. Compounds **4o** and **4p** exhibited strong cytotoxic effects against human non-tumor cell line HFF1. The *β*-lactam ureas **4a–t** were estimated to be soluble and membrane permeable, moderately lipophilic molecules (log$P \leq 4.6$) with a predisposition to be CYP3A4 and P-glycoprotein substrates. The tools PASS and SwissTargetPrediction could not predict biological targets for compounds **4a–t** with high probability, pointing to the novelty of their structure. Considering low toxicity risk, molecules **4a** and **4f** can be selected as the most promising candidates for further structure modifications.

Keywords: (±)-*trans*-*β*-lactam ureas, antiproliferative activity, *in silico* ADMET prediction, *in silico* biological profiling

INTRODUCTION

The azetidin-2-ones, also well known as *β*-lactams, are four-membered cyclic amides (1, 2). They are an important class of compounds in medicinal chemistry due to their

*Correspondence; e-mail: Marin.Roje@irb.hr

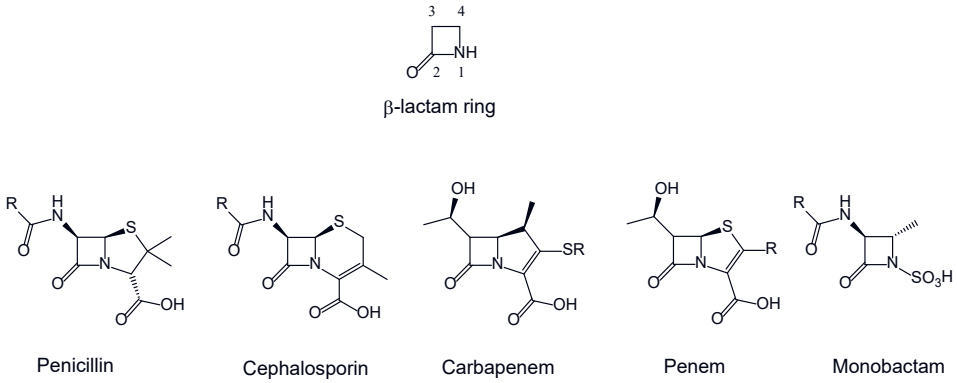

Fig. 1. Structure of β-lactam ring and the representatives of the five major categories of β-lactam antibiotics.

numerous therapeutic applications. The β-lactam ring is the key structural component of the most widely used class of β-lactam antibiotics (Fig. 1) (3), such as penicillins (4), cephalosporins (5), carbapenems, monobactams and penems (1, 6–8), which have been widely employed chemotherapeutic agents to treat bacterial infections in humans (9) and other microbial diseases (8, 10). In addition to their antibiotic activity, β-lactams demonstrate numerous other interesting pharmacological activities (10–14), such as cholesterol absorption inhibitors (15), thrombin inhibitors (16), human cytomegalovirus protease inhibitors (17), tryptase and chymase inhibitors (12), and vasopressin V1a antagonists (18). β-lactams also exhibit anticancer (19, 20), antitubercular (21), anti-HIV (22), anti-inflammatory (23), antihyperglycemic (24), antimalarial (25), and other biological activities (11, 12).

Many methods have been reported in the literature for the synthesis of β-lactams (11, 26, 27). The Staudinger reaction, [2+2] ketene-imine cycloaddition reaction, is the most frequently used method for the synthesis of β-lactam derivatives since the starting materials are readily available (12, 28). This reaction involves cyclocondensation between ketene, generated *in situ* by treatments of acid chloride (or equivalent) with an imine, in the presence of a mild base (tertiary amine) (28, 29). The reaction produces two new stereocenters (C3 and C4 in the β-lactam ring), so the β-lactam product can be *cis*-, *trans*- or a mixture of *cis*- and *trans*- isomers depending on the reactants and reaction conditions (11, 28, 30). The Staudinger reaction involves a sequential formation of the N1–C2 and C3–C4 covalent bonds of the β-lactam ring (26, 31).

Another common method of synthesising β-lactams is ester enolate-imine cyclocondensation, also called the Gilman-Speeter reaction (11, 31). However, other notable methods are sometimes employed, including the Kinugasa reaction (26, 32), photoinduced rearrangements (33), oxidative amidation (26, 34), and radical cyclisations (35).

Recently, we reported on the synthesis, separation, and absolute configuration determination of 3-amino-β-lactams (36). In that study, 3-amino-β-lactams were prepared by ester enolate/imine cyclocondensation. This method afforded diastereomerically and enantiomerically pure chiral 3-amino-β-lactams possessing *p*-fluorophenyl and *p*-methoxyphenyl

substituents at N1 and C4 positions, having a similar structure as ezetimibe, the cholesterol absorption inhibitor.

In the present study, a series of novel (±)-*trans*-*β*-lactam ureas **4a–t** were synthesized and evaluated for their antibacterial and antifungal activities *in vitro*. The compounds **4a**, **4b**, **4c**, **4f**, **4h**, **4n**, **4o**, **4p**, and **4s** were evaluated for their antiproliferative activity *in vitro* against normal and several types of cancer cell lines. In addition, drug-likeness, ADMET prediction, and biological profiling studies were carried out using *in silico* tools.

EXPERIMENTAL

General

All needed chemicals were purchased from commercial suppliers Merck (Germany), Fluka (Switzerland) and Kemika (Croatia). Dichloromethane, ethanol, and acetonitrile were dried prior to use according to standard methods. HPLC-grade acetonitrile and methanol were purchased from Honeywell (Germany). Thin layer chromatography (TLC) was carried out on silica gel F254 analytical sheets (DC-Alufolien-Kieselgel F254, Merck KGaA, Germany). Visualization of TLC plates was carried out under ultra-violet irradiation (254 nm) or by ninhydrin. Flash column chromatography was carried out using silica gel Si60 (particle size, 0.04–0.063 mm, 230–400 mesh (Merck).

Melting points were determined using an Olympus BX51 polarising microscope equipped with a Linkam TH600 hot stage and PR600 temperature controller and the Olympus C 5050 ZOOM digital camera (Olympus, Japan).

^{1}H and ^{13}C NMR spectra were recorded on Bruker AV 600 (^{1}H 600 MHz and ^{13}C 151 MHz) spectrometers (Bruker Technologies, Germany) in deuterated chloroform ($CDCl_3$) at ambient temperature. Chemical shifts (δ) were expressed in parts per million (ppm) relative to tetramethylsilane (TMS) as an internal standard. All of the coupling constants (J) are given in hertz (Hz). Splitting patterns were reported as s, singlet; d, doublet; t, triplet; p, pentet; h, heptet; m, multiplet; bs, broad singlet; dd, doublet of doublets and tdd, triplet of doublet of doublets.

FTIR-ATR spectra were recorded using a Fourier-transform infrared attenuated total reflection PerkinElmer UATR Two (PerkinElmer, USA) spectrometer in the range 450 to 4000 cm^{-1}.

Electrospray ionisation quadrupole-time-of-light high-resolution mass spectrometric (ESI-Q-TOF-HRMS) experiments were performed with Agilent 1290 infinity II/6550 Q-TOF (Agilent Technologies, Germany) instrument.

RP-HPLC analyses were performed on an Agilent 1200 Series System (Agilent Technologies, Germany), equipped with a vacuum degasser, a quaternary pump, a thermostated column compartment, an autosampler, and a variable wavelength detector. RP-HPLC analysis for the determination of the *cis*/*trans* ratio of 3-phthalimido-*β*-lactam **2a**/**2b** and analysis of compound 3-amino-*β*-lactam **3** was performed on Symmetry C18 (150 × 4.6 mm, 5 μm, Waters, USA) column. The method used was as follows: water (eluent A), acetonitrile (eluent B); 0–15 min gradient: 30 to 70 % eluent B; 15–18 min isocratic: 70 % eluent B; 18.01–21 min isocratic: 30 % B; flow: 1 mL min^{-1}, detection wavelength: 254 nm, column temperature: 30 °C, injection volume: 20 μL.

RP-HPLC analyses of racemic trans-β-lactam ureas **4a–t** were performed on a Synergi Polar-RP 80A (150 mm × 4.6 mm, 4 μm, Phenomenex, USA) column using a gradient elution of (A) water + 0.1 % trifluoroacetic acid and (B) acetonitrile as follows: 0–10 min, 50–100 % B; 10–13 min, 100 % B; 13.01–17 min 50 % B; flow rate 1.0 mL min^{-1}. The column temperature was maintained at 30 °C and the sample injection volume was 20 μL. The UV detection was carried out at 254 nm.

*Synthesis of (4-fluorophenyl)[(4-methoxyphenyl)methylene]imine (**1**)*

To a solution of 4-methoxybenzaldehyde (6 mL, 49.313 mmol) in dry dichloromethane (30 mL) at room temperature, 4-fluoroaniline (4.67 mL, 49.313 mmol) was added, followed by activated 4-Å molecular sieves powder (2 g). The reaction mixture was stirred at room temperature for 20 h. Then the mixture was filtered through a short layer of Celite (rinsed with dichloromethane) to remove the molecular sieves. The filtrate was concentrated under reduced pressure to afford crude imine as oil. Pure imine **1** (8.1 g, 73 %) was obtained as white crystals after recrystallization from ethyl acetate and hexane.

Synthesis of cis/trans*-3-phthalimido-β-lactam (**2*****a***/**2*****b***)*

A suspension of phthalimidoacetic acid (4.03 g, 19.629 mmol) in dry dichloromethane (150 mL) was cooled to 0 °C under an argon atmosphere. 2-Chloro-1-methylpyridinium iodide (6.69 g, 39.258 mmol) was then added, followed by triethylamine (10.9 mL, 78.516 mmol). The mixture was stirred for 2 hours maintaining the same temperature. Imine **1** (3.0 g, 13.086 mmol) in dry dichloromethane (25 mL) was then added dropwise to this mixture at the same temperature, and stirring was continued for another 2 hours at 0 °C to room temperature. After that, the mixture was refluxed for 20 hours and monitored by TLC and HPLC. After completion of the reaction, the reaction mixture was washed with saturated sodium bicarbonate solution (150 mL), saturated sodium chloride solution (150 mL) and deionized water (150 mL). The organic layer was dried over anhydrous sodium sulfate, filtered, and evaporated to obtain the crude product. The *cis*/*trans* ratio in the crude product was 1:5. Column chromatography over silica gel was performed using chloroform/dichloromethane/ethyl acetate mixture (7:1:1) to isolate *cis*- and *trans*-3-phthalimido-β-lactams in pure forms.

*Synthesis of 3-amino-β-lactam (**3**)*

Ethylenediamine (1.21 mL, 18.156 mmol) was added to a suspension of *trans*-3--phthalimido-β-lactam (**2b**) (3.78 g, 9.078 mmol) in dry ethanol (100 mL) under argon atmosphere. The mixture was stirred at 65 °C and the progress of the reaction was monitored by TLC. After completion of the reaction (1 hour), the ethanol was evaporated under reduced pressure, and the crude mass was dissolved in ethyl acetate (200 mL). The solution was washed with saturated sodium chloride solution (100 mL) and deionised water (100 mL). The organic layer was dried over anhydrous sodium sulfate, filtered, and concentrated under reduced pressure to obtain the crude product which was then purified by column chromatography over silica gel using ethyl acetate as the eluent solvent. The product **3** was obtained as a white solid.

*General procedure for the synthesis of (±)-*trans*-β-lactam ureas (**4a–t**)*

To a solution of (±)-*trans*-3-amino-β-lactam [(±)-**3**] (50 mg, 0.175 mmol) in dry acetonitrile (5 mL) the appropriate isocyanate (**4a–t**) (0.263 mmol) was added and the reaction mixture was stirred for 20 hours at room temperature. Then the solvent was concentrated under reduced pressure and the obtained crude product was further purified by column chromatography over silica gel using hexane/ethyl acetate = 4:1 as the eluent. The pure *trans*-β-lactam ureas were obtained after trituration with hexane in good to excellent yields (75–98 %). The structure of target compounds **4a–t** was ascertained by spectroscopic methods such as FT-IR, ^{1}H NMR, ^{13}C NMR, and mass spectrometry.

Physicochemical and spectral data for compounds **1**, **2**, **3**, **4a–t** are given in Tables I and II. The ^{1}H NMR, ^{13}C NMR, FT-IR spectra, and HPLC chromatograms of compounds **1**, **2**, **3**, **4a–t** are shown in the Supplementary materials (Figs. S1 to S112).

Antibacterial activity

The antibacterial activity of the synthesized compounds was evaluated by broth microdilution assay according to the CLSI guidelines (37) with minor modifications using *Escherichia coli* NCTC 12241 (National Collection of Type Cultures, Salisbury, UK), *Staphylococcus aureus* ATCC 6538 (American Type Culture Collection, Manassas, Virginia, USA), and *Pseudomonas aeruginosa* NCTC 12903 as indicator strains. Referent compounds used in the laboratory were: chloramphenicol (Merck&Co., USA), norfloxacin (Merck&Co.), and amikacin (Merck&Co.).

Stock solutions were made at 6.4 mg mL^{-1} (*m*/*V*) using DMSO and were diluted with cation-adjusted Mueller Hinton broth (CAMHB) culture media to be tested at a final concentration of 128–0.125 μg mL^{-1} (prepared by serial two-fold dilutions along the rows of a microtitre plate). Fresh overnight growth of bacteria at 37 °C on tryptic soy agar was used to prepare inocula of 0.5 MacFarland concentration by turbidity adjustment in sterile 5 mL physiological saline (0.85 % NaCl). Inocula were subsequently diluted with CAMHB to reach a final concentration of 5×10^4 CFU per well of a microtitre plate in a total volume of 100 μL per well. All tests were performed on two independent occasions each time in technical duplicates. Each experimental run included positive (drug-free and sample-free wells, *i.e.*, bacteria and sterile media only) and negative (sterile media only) controls and quality control using chloramphenicol. All assays were performed at 35 °C aerobically. Results were interpreted both visually and spectrophotometrically at 600 nm using a microplate reader, and minimal inhibitory concentrations (*MIC*) (38), if observed, were screened by culture isolation from the wells, including any available higher concentrations, for evaluating minimal bactericidal concentration (*MBC*).

Antifungal activity

Antifungal activity of newly synthesized *trans*-β-lactam ureas **4a–t** was determined by the method of microdilution in broth according to CLSI guidelines (39) on strains of *Candida albicans* ATCC 90028 and *Saccharomyces cerevisiae* BY 4741 ATCC 4040002. All synthesized *trans*-β-lactam ureas **4a-t** were prepared for antibacterial activity testing except

that the YPD broth and agar culture media used were incubated for 48 hours at 30 ± 1 ° C and the wells of the microtiter plate were inoculated at a concentration of 5×10^3 CFU mL^{-1}. The antifungal agent nystatin was used for quality control.

Antiproliferative activity

Antiproliferative activity was studied on selected compounds **4a**, **4b**, **4c**, **4f**, **4h**, **4n**, **4o**, **4p**, and **4s** (Fig. S113). The reason for this selection is due to the fact that only selected *β*-lactam ureas can undergo further transformation into 5-membered hydantoins, our next synthetic targets currently in preparation. The above-mentioned compounds were tested on three human cell lines: HepG2 (liver hepatocellular carcinoma, HB 8065, from ATCC), A2780 (ovarian carcinoma, 93112519, from ECACC, Porton Down, UK), MCF7 (breast adenocarcinoma, HTB-22, from ATCC) and one human non-tumor cell line HFF1 (untransformed human fibroblasts, SCRC-1041, from ATCC) by the MTT assay (40, 41). The cells were cultured as monolayers and maintained in different media [Dulbecco's modified Eagle's medium (DMEM) or Roswell Park Memorial Institute (RPMI-1640) medium] containing different concentrations of fetal bovine serum (FBS). The A2780 cancer cells were cultured in RPMI-1640 medium with 10 % FBS. The MCF7 carcinoma cells were cultured in DMEM supplemented with 10 % FBS and insulin (0.01 mg mL^{-1}). The HepG2 cell lines were cultured in DMEM supplemented with 10 % FBS and HFF1 cells in DMEM containing 15 % FBS. All cell lines were maintained in a humidified atmosphere with 5 % CO_2 at 37 °C.

The growth inhibition activity was assessed according to the slightly modified procedure of the National Cancer Institute, Developmental Therapeutics Program (42). The cells were inoculated onto standard 96-well microtiter plates on day 0. The cell concentrations were adjusted according to the cell population doubling time (PDT): 9.6×10^3 per mL for HepG2, A2780, 1.3×10^4 per mL for MCF7, and 1.6×10^3 per mL for HFF1 cell lines. Stock solutions of all the compounds were prepared in DMSO at a concentration of 0.04 mol L^{-1}. The following day, the cells were treated with various concentrations of compounds **4a**, **4b**, **4c**, **4f**, **4h**, **4n**, **4o**, **4p**, and **4s** (from 10^{-8} to 10^{-4} mol L^{-1} in duplicate), and incubated for further 72 hours at 37 °C with 5 % CO_2. The working dilutions in DMSO were freshly prepared on the day of testing. After 72 h of incubation, the cell growth rate was evaluated by performing the MTT assay, which detects dehydrogenase activity in viable cells. The MTT cell proliferation assay is a colorimetric assay system, which measures the reduction of tetrazolium component (MTT) into an insoluble formazan product by the mitochondria of viable cells. For this purpose, the substance-treated medium was discarded and 40 μL of MTT reagent was added to each well at a concentration of 0.5 mg mL^{-1}. After four hours of incubation, the precipitates were dissolved in 160 μL of DMSO. The absorbance (A) was measured on a microplate reader at 595 nm (Hidex Chameleon V). The percentage of growth (PG) of the cell lines was calculated according to one or the other of the following two expressions:

if (mean A_{test} – mean A_{tzero}) ≥ 0, then

$$PG = 100 \times (\text{mean } A_{test} - \text{mean } A_{tzero}) / (\text{mean } A_{ctrl} - \text{mean } A_{tzero})$$

or

if (mean A_{test} – mean A_{tzero}) < 0, then

$$PG = 100 \times (\text{mean } A_{test} - \text{mean } A_{tzero})/A_{tzero}$$

where the mean A_{tzero} is the average of the absorbance measurements before the exposure of the cells to the test compound, the mean A_{test} is the average absorbance after the desired period, and the mean A_{ctrl} is the average absorbance after the desired period with no exposure of the cells to the test compound. Each test was performed in quadruplicate in two individual experiments. The results are expressed as IC_{50}, which is the concentration necessary for 50 % inhibition. The IC_{50} values for each compound were calculated from concentration-response curves using linear regression analysis by fitting the test concentrations that give PG values above and below the reference value (*i.e.*, 50 %). However, if for a given cell line all of the tested concentrations produce PGs exceeding the respective reference level of effect (*e.g.*, PG value of 50), then the highest tested concentration is assigned as the default value, which is preceded by a ">" sign.

*Drug-likeness and ADMET of compounds **4a–t***

The program ADMET (absorption, distribution, metabolism, excretion, and toxicity) Predictor ver. 9.5 (Simulation Plus Inc., USA) (43) was used to predict the simple structural features: the number of hydrogen bond donors (HBD) and acceptors (HBA), topological polar surface area (TPSA) and physicochemical properties: water solubility (Sw), lipophilicity coefficient (log*P*), human effective jejunal permeability (Peff) and permeability to Madin-Darby canine kidney (MDCK) cells (Table SII). In addition, the following pharmacokinetic parameters were calculated: percent unbound to blood plasma proteins in humans (hum_fup%), percent unbound in human liver microsomes (fumic%), qualitative estimation of the probability of passing through the blood-brain barrier (BBB), the brain/blood partition coefficient (logBB), the likeness of P-glycoprotein efflux (Pgp sub) and inhibition (Pgp inh) as well as toxicity related parameters (rodent chronic toxicity Rat_and Mouse_TD50 values estimating an oral dose, in mg kg^{-1} per day) of a compound required to induce tumors in 50 % of a rat/mouse population after exposure over a standard lifetime, qualitative estimation of the likelihood of the hERG potassium channel inhibition in human (hERG_filter), potential toxicity liabilities summarizing all ADMET risk models (Tox_Code). The web tool admetSAR (http://lmmd.ecust.edu.cn/admetSAR2) was used to predict whether a compound may be an inhibitor (CYPs 3A4, 2D6, 2C19, 2C9 and 1A2) or a substrate (CYPs 3A4, 2D6 and 3A4) of the CYP enzymes (Table SII) (44).

*Target determination for compounds **4a–t** by PASS and SwissTargetPrediction*

The biological profiles of the new *trans*-*β*-lactam ureas **4a–t** were estimated by the machine-learning-based software PASS 2020 (Prediction of activity spectra for substances) (45). The PASS biological screening involved 1,945 PASS-recommended activities including pharmacological effects, mechanisms of action, toxic and adverse effects, antitargets, metabolism-related actions, gene expression regulation, and transporters-related actions. The biological profile is provided as a set of predicted activities along with the associated probabilities of being active (Pa) and inactive (Pi), and with the criteria Pa > Pi and Pa > 0.3, > 0.5 and 0.7 (Table SIII). The SwissTargetPrediction web server (46) was also used to predict potential targets for *trans*-*β*-lactam ureas **4a–t**, based on structural similarity to already known actives. The SMILES (simplified molecular input line entry system) strings of the compounds served as input to all used computational tools.

RESULTS AND DISCUSSION

The synthesized new β-lactam urea structures fall into the category of monobactams, where the β-lactam ring is monocyclic. This moiety is mainly responsible for the antibacterial properties, as it can block bacterial cell wall synthesis through its covalent binding to penicillin-binding proteins (PBPs) (12).

Most chemical modifications commonly made to β-lactam antibiotics involve functionalization of the pharmacophore core, which comprises all four positions of the β-lactam ring. In our study, we have considered the introduction of different substituent groups at positions 2 and 3 (ureido and aromatic) to modulate the possibility of interactions with their targets and consequently achieve new biological activity.

Imine **1** was synthesised according to our recent work; substituents at the N1 and C4 positions of the β-lactam ring are the same as in the ref. 36. Novelty of the current work is restricted to urea moiety and lies in the subsequent derivatization of the NH_2 group of β-lactam to yield new structures.

Chemistry

The novel *trans*-β-lactam ureas **4a–t** were synthesised as indicated in Scheme 1. In the first step, imine **1** was synthesised by a condensation reaction of 4-methoxybenzaldehyde and 4-fluoroaniline in dry dichloromethane in the presence of 4-Å powdered molecular sieves (36). Pure imine **1** was isolated in the 73 % yield after crystallisation from the ethyl acetate/hexane mixture. Imine **1** was then treated with *N*-phthalimidoglycine in the presence of triethylamine and 2-chloro-1-methylpyridinium iodide (Mukaiyama reagent) to afford a (±)-3-phthalimido-β-lactam (**2a**/**2b**) (47). The crude reaction mixture was analyzed by ^{1}H NMR spectroscopy, which clearly showed the presence of two isomeric β-lactams, in a ratio of ca. 1:5 (*cis:trans*). Conducted HPLC analysis also corroborates this finding. The ^{1}H NMR spectrum of the protons H-3 and H-4 of 3-phthalimido-β-lactam mixture (±)-**2a**/**2b** is shown in Fig. S1 (see Supplementary materials).

For the *cis* stereoisomer, the two protons H-4 and H-3 in the β-lactam ring have appeared as two doublets at 5.42 ppm and 5.65 ppm. The *cis* vicinal coupling constants were both 5.5 Hz. The corresponding coupling constant for the *trans* isomer was determined as J = 2.6 Hz, which appeared as two doublets at 5.28 and 5.31 ppm. Based on these data, the structures of the expected diastereomeric β-lactams *cis*-**2a** and *trans*-**2b** were confirmed (Scheme 1). Since the ketene generated *in situ* from *N*-phthalimidoglycine and triethylamine is a Sheehan ketene, it has a preference to form *trans*-β-lactam (28). These diastereoisomers were separated by flash-column chromatography yielding pure *trans*-β--lactam **2b** (75 %) and pure *cis*-β-lactam **2a** (11 %).

In the subsequent step, deprotection of the bulky phthalimide group of compound **2b** with ethylenediamine in dry ethanol afforded a free amine, (±)-3-amino-β-lactam (**3**), in good yield (Scheme 1) (47). The treatment of compound **3** with various aliphatic and aromatic isocyanates **4a–t** in dry acetonitrile at room temperature resulted in the isolation of β-lactam ureas **4a–t** (Scheme 1) (48). Products were isolated in good to excellent yields varying from 75 to 98 %. For physicochemical and spectral data see Tables I and II and Figs. S1 to S112.

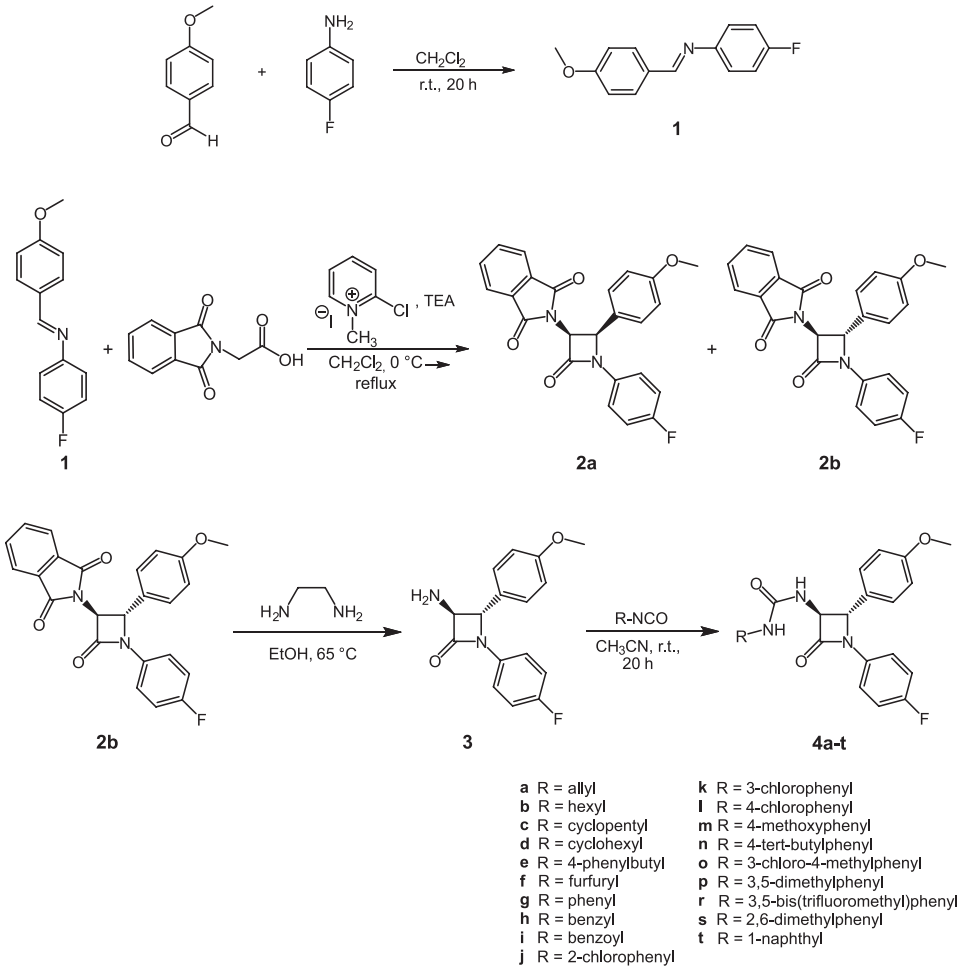

Scheme 1

In the IR spectra of compounds **4a–t** absorption peaks at 3311–3396 cm^{-1} (N–H stretch), 2918–2961 cm^{-1} (aromatic C-H stretch), 2838–2858 cm^{-1} (aliphatic C–H stretch), 1732–1756 cm^{-1} (C=O of β-lactam), 1507–1509 cm^{-1} (ring C=C stretch), 1426 and 1426 cm^{-1} (C–N stretch), 1246–1255 cm^{-1} (C–O stretch), 1224–1229 cm^{-1} (C–F stretch), 1031–1034 cm^{-1} (saturated C-O stretch) and 830–841 cm^{-1} (ring vibration due to *para*-disubstituted benzene) were observed. The IR spectra were dominated by the very strong C=O band, whereas the fingerprint region was characterised by weak IR intensities.

Physicochemical and spectral data of all compounds are given in Tables I and II.

Table I. Chemical names, molecular formula, yields, melting points and R_f *values of compounds* ***1***, ***2***, ***3***, ***4a–t***

Compd.	Chemical name	Molecular formula	Relative molecular mass (M_r)	Yield (%)	M.p. (°C)	R_f values[a]
1	(4-fluorophenyl)[(4-methoxyphenyl)methylene]amine	$C_{14}H_{12}FNO$	229.2496	73	68–70	–
2a	(±)-*cis*-1-(4-fluorophenyl)-2-(4-methoxyphenyl)-4-oxoazetidin-3-yl isoindoline-1,3-dione	$C_{24}H_{17}FN_2O_4$	416.1171	11	194.1–198.8	0.59
2b	(±)-*trans*-1-(4-fluorophenyl)-2-(4-methoxyphenyl)-4-oxoazetidin-3-yl isoindoline-1,3-dione	$C_{24}H_{17}FN_2O_4$	416.1171	75	197.3–198.8	0.71
3	3-amino-1-(4-fluorophenyl)-4-(4-methoxyphenyl)azetidin-2-one	$C_{16}H_{15}FN_2O_2$	286.3009	67	98.7–101.2	0.39
4a	1-allyl-3-[(±)-*trans*-1-(4-fluorophenyl)-2-(4-methoxyphenyl)-4-oxoazetidin-3-yl]urea	$C_{20}H_{20}FN_3O_3$	369.1489	89	86.1–88.5	0.22
4b	1-hexyl-3-((±)-*trans*-1-(4-fluorophenyl)-2-(4-methoxyphenyl)-4-oxoazetidin-3-yl]urea	$C_{23}H_{28}FN_3O_3$	413.2115	89	58.3–62.4	0.32
4c	1-cyclopentyl-3-[(±)-*trans*-1-(4-fluorophenyl)-2-(4-methoxyphenyl)-4-oxoazetidin-3-yl]urea	$C_{22}H_{24}FN_3O_3$	397.1802	86	138.7–143.7	0.30
4d	1-cyclohexyl-3-[(±)-*trans*-1-(4-fluorophenyl)-2-(4-methoxyphenyl)-4-oxoazetidin-3-yl]urea	$C_{23}H_{26}FN_3O_3$	411.1958	84	127.8–129.4	0.40
4e	1-[(±)-*trans*-1-(4-fluorophenyl)-2-(4-methoxyphenyl)-4-oxoazetidin-3-yl]-3-(4-phenylbutyl)urea	$C_{27}H_{28}FN_3O_3$	461.2115	79	86.7–87.1	0.33
4f	1-[(±)-*trans*-1-(4-fluorophenyl)-2-(4-methoxyphenyl)-4-oxoazetidin-3-yl]-3-(furan-2-ylmethyl)urea	$C_{22}H_{20}FN_3O_4$	409.1438	90	188.8–189.9	0.22
4g	1-phenyl-3-[(±)-*trans*-1-(4-fluorophenyl)-2-(4-methoxyphenyl)-4-oxoazetidin-3-yl]urea	$C_{23}H_{20}FN_3O_3$	405.1489	94	116.5–117.1	0.29
4h	1-benzyl-3-[(±)-*trans*-1-(4-fluorophenyl)-2-(4-methoxyphenyl)-4-oxoazetidin-3-yl]urea	$C_{24}H_{22}FN_3O_3$	419.1645	90	164.1–167.3	0.28

Compd.	Chemical name	Molecular formula	Relative molecular mass (M_r)	Yield (%)	M.p. (°C)	R_f values[a]
4i	1-benzoyl-3-[(±)-*trans*-1-(4-fluorophenyl)-2-(4-methoxyphenyl)-4-oxoazetidin-3-yl]urea	$C_{24}H_{20}FN_3O_4$	433.1438	90	225.5–227.8	0.54
4j	1-(2-chlorophenyl)-3-[(±)-*trans*-1-(4-fluorophenyl)-2-(4-methoxyphenyl)-4-oxoazetidin-3-yl]urea	$C_{23}H_{19}ClFN_3O_3$	439.1099	98	215.4–216.2	0.64
4k	1-(3-chlorophenyl)-3-[(±)-*trans*-1-(4-fluorophenyl)-2-(4-methoxyphenyl)-4-oxoazetidin-3-yl]urea	$C_{23}H_{19}ClFN_3O_3$	439.1099	92	116.1–119.2	0.34
4l	1-(4-chlorophenyl)-3-[(±)-*trans*-1-(4-fluorophenyl)-2-(4-methoxyphenyl)-4-oxoazetidin-3-yl]urea	$C_{23}H_{19}ClFN_3O_3$	439.1099	89	215.3–217.8	0.32
4m	1-[(±)-*trans*-1-(4-fluorophenyl)-2-(4-methoxyphenyl)-4-oxoazetidin-3-yl]-3-(4-methoxyphenyl)urea	$C_{24}H_{22}FN_3O_4$	435.1594	93	109.3–110.1	0.22
4n	1-[4-(*tert*-butyl)phenyl]-3-[(±)-*trans*-1-(4-fluorophenyl)-2-(4-methoxyphenyl)-4-oxoazetidin-3-yl]urea	$C_{27}H_{28}FN_3O_3$	461.2115	91	195.4–196.0	0.47
4o	1-(3-chloro-4-methylphenyl)-3-[(±)-*trans*-1-(4-fluorophenyl)-2-(4-methoxyphenyl)-4-oxoazetidin-3-yl]urea	$C_{24}H_{21}ClFN_3O_3$	453.1255	87	174.2–178.8	0.41
4p	1-(3,5-dimethylphenyl)-3-[(±)-*trans*-1-(4-fluorophenyl)-2-(4-methoxyphenyl)-4-oxoazetidin-3-yl]urea	$C_{25}H_{24}FN_3O_3$	433.1802	90	163.2–164.2	0.44
4r	1-[3,5-bis(trifluoromethyl)phenyl]-3-[(±)-*trans*-1-(4-fluorophenyl)-2-(4-methoxyphenyl)-4-oxoazetidin-3-yl]urea	$C_{25}H_{18}F_7N_3O_3$	541.1236	75	192.8–193.7	0.43
4s	1-(2,6-dimethylphenyl)-3-[(±)-*trans*-1-(4-fluorophenyl)-2-(4-methoxyphenyl)-4-oxoazetidin-3-yl]urea	$C_{25}H_{24}FN_3O_3$	433.1802	89	127.2–128.9	0.30
4t	1-[(±)-*trans*-1-(4-fluorophenyl)-2-(4-methoxyphenyl)-4-oxoazetidin-3-yl]-3-(naphthalen-1-yl)urea	$C_{27}H_{22}FN_3O_3$	455.1645	84	218.3–219.4	0.40

[a] Eluent: **2a**, **2b** (chloroform/dichloromethane/ethyl acetate = 7:1:1); **3** (ethyl acetate); **4a**–**t** (chloroform/ethyl acetate = 4:1).

Table II. Spectral data of compounds ***1***, ***2***, ***3*** *and* ***4a–t***

Compd.	FTIR-ATR ($\tilde{\nu}$/cm^{-1})	^{1}H NMR (600 MHz, $CDCl_3$) (δ/ppm)	^{13}C NMR (151 MHz, $CDCl_3$) (δ/ppm)	HRMS $(M+H)^+$
1	2925, 2847, 1626, 1604, 1512, 1458, 1308, 1253, 1208, 1179, 1159, 1021, 841	3.86 (s, 3 H), 6.97 (d, J = 8.8 Hz, 2 H), 7.06 (t, $J_{1,2}$ = 8.7 Hz, 2 H), 7.12–7.21 (m, 2 H), 7.83 (d, J = 8.7 Hz, 2 H), 8.35 (s, 1 H)	55.55, 114.34, 115.91 (d, J = 22.4 Hz), 122.34 (d, J = 8.1 Hz), 129.25, 130.6, 148.50 (d, J = 2.7 Hz, 4-FC6H4), 159.63, 160.97 (d, J = 244.1 Hz), 162.74	– [a]
2a	2895, 1781, 1756, 1721, 1611, 1510, 1467, 1442, 1385, 1254, 1175, 1115, 1053, 956, 832, 814, 750, 716	3.66 (s, 3 H), 5.42 (d, J = 5.5 Hz, 1 H), 5.65 (d, J = 5.5 Hz, 1 H), 6.72 (d, J = 8.8 Hz, 2 H), 7.02 (t, J = 8.7 Hz, 2 H), 7.17 (d, J = 8.7 Hz, 2 H), 7.38–7.48 (m, 2 H), 7.61–7.77 (m, 4 H)	55.28, 59.27, 60.97, 114.16, 116.14 (d, J = 22.8 Hz), 118.98 (d, J = 7.9 Hz), 123.67, 128.67, 131.33, 133.80 (d, J = 2.7 Hz), 134.43, 159.53 (d, J = 244.2 Hz), 159.75, 160.85, 166.85	417.1255
2b	3007, 2932, 2836, 1778, 1754, 1713, 1612, 1507, 1467, 1369, 1311, 1253, 1229, 1180, 1148, 1120, 1105, 1034, 970, 941, 833, 717, 530	3.81 (s, 3 H), 5.28 (d, J = 2.6 Hz, 1 H), 5.31 (d, J = 2.6 Hz, 1 H), 6.88–7.01 (m, 4 H), 7.27–7.36 (m, 4 H), 7.73–7.80 (m, 2 H), 7.84–7.91 (m, 2 H)	55.49, 61.33, 63.12, 115.02, 116.05 (d, J = 22.8 Hz), 119.31 (d, J = 8.0 Hz), 123.96, 127.44, 127.70, 131.82, 133.56 (d, J = 2.8 Hz), 134.73, 159.54 (d, J = 244.1 Hz), 160.46, 162.12, 166,95	417.1248
3	3384, 3341, 3177, 2933, 2840, 1732, 1611, 1510, 1483, 1380, 1246, 1229, 1154, 1115, 1029, 965, 832, 793, 717	1.82 (bs, 2 H), 3.80 (s, 3 H), 4.04 (d, J = 2.2 Hz, 1 H), 4.60 (d, J = 2.2 Hz, 1 H), 6.84–6.98 (m, 4 H), 7,20–7,30 (m, 4 H)	55.46, 66.58, 70.21, 114.73, 115.98 (d, J = 22.6Hz), 118.96 (d, J = 7.9 Hz), 127.33, 128.55, 133.78 (d, J = 2.8 Hz), 159.24 (d, J = 243.6 Hz), 160.04, 168.01	287.1183
4a	3346, 2933, 2838, 1 745, 1636, 1612, 1560, 1507, 1426, 1288, 1247, 1224, 1175, 1137, 1102, 923, 830	3.67–3.78 (m, 2 H), 3.79 (s, 3 H), 4,42 (dd, J_1 = 6.8 Hz, J_2 = 2,3 Hz, 1 H), 5.01 (d, J = 2,3 Hz, 1 H), 5.07 (dd, J_1 = 10.3 Hz, J_2 = 1.5 Hz, 1 H), 5.16 (dd, J_1 = 17.2 Hz, J_2 = 1.6 Hz, 1 H), 5.37 (t, J_1 = J_2 = 5,8 Hz, 1 H), 5.74–5.84 (m, 1 H), 6.04 (d, J = 6.8 Hz, 1 H), 6.84–6.92 (m, 4 H), 7.17–7.25 (m, 4 H)	42.94, 55.46, 63.95, 67.24, 114.76, 115.96, 115.98 (d, J = 22.8 Hz), 119.26 (d, J = 7.9 Hz), 127.59, 128.19, 133.57 (d, J = 2.7 Hz), 135.14, 157.46, 159.41 (d, J = 244.5 Hz), 160.08, 166.34.	370.1579
4b	3352, 2956, 2929, 2858, 1748, 1639, 1563, 1507, 1386, 1247, 1226, 1175, 1136, 1031, 830	0.83–0.90 (m, 3 H), 1.19–1.32 (m, 6 H), 1.43 (p, J = 7.2, 2 H), 3.00–3.16 (m, 2 H), 3.79 (s, 3 H), 4.40 (dd, J_1 = 6.7 Hz, J_2 = 2.3 Hz, 1 H), 5.01 (d, J = 2.2 Hz, 1 H), 5.22 (t, J_1 = J_2 = 5.6 Hz, 1 H), 5.95 (d, J = 6,7 Hz, 1 H), 6.85–6.91 (m, 4 H), 7.18–7.25 (m, 4 H)	14.16, 22.72, 26.72, 30.19, 31.66, 40.64, 55.44, 63.98, 67.29, 114.72, 115.95 (d, J = 22.7 Hz), 119.23 (d, J = 7.8 Hz), 127.57, 128.25, 133.60 (d, J = 2.7 Hz), 157.55, 159.38 (d, J = 244.0 Hz), 160.03, 166.52	414.2158

Compd.	FTIR-ATR ($\tilde{\nu}$/cm^{-1})	^{1}H NMR (600 MHz, $CDCl_3$) (δ/ppm)	^{13}C NMR (151 MHz, $CDCl_3$) (δ/ppm)	HRMS $(M+H)^+$
4c	3342, 2959, 1747, 1633, 1556, 1509, 1385, 1289, 1250, 1226, 1175, 1131, 1101, 1031, 830	1.28–1.40 (m, 2 H), 1.48–1.58 (m, 2 H), 1.58–1.67 (m, 2 H), 1.90 (tdd, J_1 = 13.2 Hz, J_2 = 10.1 Hz, J_3 = 6.2 Hz, 2 H), 3.79 (s, 3 H), 3.97 (h, J = 6.8 Hz, 1 H), 4.43 (dd, J_1 = 6,6 Hz, J_2 = 2.2 Hz, 1 H), 4.99 (d, J = 2.2 Hz, 1H), 5.09 (d, J = 7.3 Hz, 1 H), 5.74 (d, J = 6,5 Hz, 1 H), 6.85–6.93 (m, 4 H), 7.19–7.28 (m, 4 H)	23.70, 33.51, 33.61, 52.26, 55.46, 64.07, 67.32, 114.74, 115.96 (d, J = 22.6 Hz), 119.23 (d, J = 7.9 Hz), 127.60, 128.26, 133.65 (d, J = 2.4 Hz), 157.10, 159.40 (d, J = 244.0 Hz), 160.06, 166.17	398.1871
4d	3327, 2929, 2853, 1751, 1636, 1560, 1508, 1450, 1304, 1248, 1225, 1175, 1136, 1100, 1031, 830	1.02–1.17 (m, 3 H), 1.23–1.35 (m, 2 H), 1.52–1.60 (m, 1 H), 1.62–1.71 (m, 2 H), 1.83–1.94 (m, 2 H), 3.56–3.56 (m, 1 H), 3.78 (s, 3 H), 4.40 (dd, J_1 = 6.4 Hz, J_2 = 2.2 Hz, 1 H), 4.90 (d, J = 8.0 Hz, 1 H), 5.01 (d, J = 6,4 Hz, 1 H), 5.65 (d, J = 6.4 Hz, 1 H), 6.84–6.93 (m, 4 H), 7.19–7.28 (m, 4 H)	25.01, 25.04, 25.65, 33.75, 33.90, 49.27, 55.45, 64.01, 67.36, 114.72, 115.96 (d, J = 22.8 Hz), 119.23 (d, J = 7.9 Hz), 127.58, 128.28, 133.64 (d, J = 2.7 Hz), 156.67, 160.03, 159.39 (d, J = 244.0 Hz), 166.20	412.2007
4e	3349, 3026, 2932, 2858, 1750, 1634, 1562, 1508, 1426, 1387, 1250, 1228, 1175, 1140, 1102, 1031, 831	1.49 (p, J = 7.2 Hz, 2 H), 1.57–1.64 (m, 2 H), 2.60 (t, J = 7.7 Hz, 2 H), 3.05–3.23 (m, 2 H), 3.79 (s, 3 H), 4.40 (dd, J_1 = 6.6 Hz, J_2 = 2.3 Hz, 1 H), 5.00 (d, J = 2.2 Hz, 1 H), 5.04 (t, J = 5.6 Hz, 1 H), 5.71 (d, J = 6.6 Hz, 1 H), 6.83–6.92 (m, 4 H), 7.12–7.19 (m, 3 H), 7.19–7.28 (m, 6 H)	28.78, 29.86, 35.65, 40.39, 55.45, 63.96, 67.29, 114.73, 115.97 (d, J = 22.7 Hz), 119.22 (d, J = 7.9 Hz), 125.92, 127.57, 128.20, 128.46, 128.52, 133.58 (d, J = 2.7 Hz), 142.34, 157.47, 159.39 (d, J = 244.1 Hz), 160.04, 166.42	462.2175
4f	3333, 1732, 1650, 1611, 1556, 1508, 1427, 1388, 1426, 1247, 1218, 1176, 1146, 1104, 1076, 1028, 1010, 833, 743	3.79 (s, 3 H), 4.25 (dd, J_1 = 15.6 Hz, J_2 = 5.5 Hz, 1 H), 4.32 (dd, J_1 = 15.6 Hz, J_2 = 5.8 Hz, 1 H), 4.40 (dd, J_1 = 6.7 Hz, J_2 = 2.3 Hz, 1 H), 5.00 (d, J = 2.2 Hz, 1 H), 5.60 (t, J = 5.7 Hz, 1 H), 5.99 (d, J = 6.7 Hz, 1 H), 6.17 (d, J = 2.9 Hz, 1 H), 6.26 (dd, J_1 = 3.2 Hz, J_2 = 1.8 Hz, 1 H), 6.84–6.91 (m, 4 H), 7.17–7,23 (m, 4 H), 7.27–7.28 (m, 1 H)	37.43, 55.46, 63.91, 67.16, 107.19, 110.55, 114.75, 115.99 (d, J = 22.8 Hz), 119.28 (d, J = 7.9 Hz), 127.62, 128.12, 133.53 (d, J = 2.5 Hz), 142.15, 152.24, 157.18, 159.42 (d, J = 244.3 Hz), 160.09, 166.20	410.1509
4g	3328, 1741, 1654, 1599, 1551, 1508, 1441, 1386, 1309, 1187, 1175, 1130, 1102, 830, 751, 691	3.78 (s, 3 H), 4.40 (dd, J_1 = 6.8 Hz, J_2 = 2.3 Hz, 1 H), 5.07 (d, J = 2.3 Hz, 1 H), 6.35 (d, J = 6.8 Hz, 1 H), 6.82–6.90 (m, 4 H), 6.94 (t, J_1 = J_2 = 7.4 Hz, 1 H), 7.13 (t, J_1 = J_2 = 8.0 Hz, 2 H), 7.16–7.24 (m, 6 H), 7.58 (s, 1 H)	55.45, 63.73, 66.97, 114.79, 116.03 (d, J = 22.8 Hz), 119.42 (d, J = 7.9 Hz), 120.29, 123.58, 127.65, 127.88, 129.11, 133.38 (d, J = 2,7 Hz), 138.35, 155.31, 159.51 (d, J = 244.5 Hz), 160.15, 166.50	406.1550

Compd.	FTIR-ATR ($\tilde{\nu}$/cm^{-1})	^{1}H NMR (600 MHz, $CDCl_3$) (δ/ppm)	^{13}C NMR (151 MHz, $CDCl_3$) (δ/ppm)	HRMS $(M+H)^+$
4h	3358, 3264, 3035, 2965, 2929, 1735, 1646, 1555, 1506, 1425, 1384, 1243, 1176, 1155, 1105, 1022, 841, 748, 706	3.78 (s, 3 H), 4.23 (dd, J_1 = 14.9 Hz, J_2 = 5.6 Hz, 1H), 4.30 (dd, J_1 = 14.7 Hz, J_2 = 5.8 Hz, 1H), 4.38 (dd, J_1 = 6.7 Hz, J_2 = 2.3 Hz, 1 H), 4.97 (d, J = 2.3 Hz, 1 H), 5.57 (t, $J_{1,2}$ = 5.8 Hz, 1 H), 5.97 (d, J = 6.6 Hz, 1 H), 6.83–6.89 (m, 4 H), 7.14–7.25 (m, 7 H), 7.24–7.30 (m, 2 H)	44.39, 55.45, 63.93, 67.21, 114.72, 115.97 (d, J = 22.8 Hz), 119.23 (d, J = 7.9 Hz), 127.43, 127.60, 128.12, 128.73, 133.51 (d, J = 2.6 Hz), 139.01, 157.45, 159.38 (d, J = 244.0 Hz), 160.05, 166.20	420.1700
4i	3266, 2934, 2837, 1756, 1676, 1611, 1535, 1508, 1466, 1385, 1247, 1217, 1175, 1137, 1101, 1029, 1005, 831, 705	3.80 (s, 3 H), 4.69 (dd, J_1 = 7.5 Hz, J_2 = 2.5 Hz, 1 H), 5.10 (d, J = 2.4 Hz, 1 H), 6.87–6.95 (m, 4 H), 7.21–7.30 (m, 4 H), 7.29–7.36 (m, 2 H), 7.47 (t, J_1 = J_2 = 7.5 Hz, 1 H), 7.84 (d, J = 7.3 Hz, 1 H), 9.47 (d, J = 7.5 Hz, 1 H), 9.48 (s, 1 H)	55.48, 62.97, 66.51, 114.87, 116.00 (d, J = 22.8 Hz), 119.31 (d, J = 7.9 Hz), 127.62, 127.84, 128.01, 128.99, 131.84, 133.41, 133.56 (d, J = 2.6 Hz), 154.17, 159.42 (d, J = 244,0 Hz), 160.25, 163.67, 168.34	434.1510
4j	3340, 2928, 1733, 1679, 1650, 1612, 1587, 1538, 1508, 1390, 1247, 1212, 1177, 1101, 1028, 830	3.77 (s, 3 H), 4.54 (dd, J_1 = 6.5 Hz, J_2 = 2.2 Hz, 1 H), 5.08 (d, J = 2.2 Hz, 1 H), 6.78–6.94 (m, 6 H), 7.11 (t, J = 7.8 Hz, 1 H), 7.21–7.26 (m, 5 H), 7.45 (s, 1 H), 8.04 (d, J = 8.2 Hz, 1 H)	55.44, 63.92, 66.92, 114.79, 116.03 (d, J = 22.8 Hz), 119.41 (d, J = 7.9 Hz), 121.41, 122.80, 123.70, 127.64, 127.70, 127.78, 129.16, 133.31 (d, J = 2.5 Hz), 135.37, 154.48, 159.55 (d, J = 244.4 Hz), 160.15, 166.98	440.1162
4k	3323, 3080, 2933, 1739, 1658, 1610, 1592, 1544, 1508, 1388, 1248, 1225, 1187, 1101, 1075, 830	3.79 (s, 3 H), 4.38 (dd, J_1 = 6.9 Hz, J_2 = 2.3 Hz, 1 H), 5.12 (d, J = 2.3 Hz, 1 H), 6.58 (d, J = 6.9 Hz, 1 H), 6.82–6.90 (m, 5 H), 6.98 (t, J = 8.0 Hz, 1 H), 6.99–7.03 (m, 1 H), 7.16–7.22 (m, 4 H), 7,32 (t, J = 2.0 Hz, 1 H), 7.85 (s, 1 H)	55.46, 63.66, 66.84, 114.87, 116.14 (d, J = 22.8 Hz), 117.44, 119.35, 119.52 (d, J = 7.9 Hz), 123.14, 127.56, 127.61, 129.86, 133.13 (d, J = 2.6 Hz), 134.55, 139.69, 155.01, 159.64 (d, J = 244.6 Hz), 160.45, 166.88	440.1152
4l	3385, 3305, 2927, 1746, 1663, 1609, 1551, 1508, 1389, 1312, 1289, 1250, 1175, 1140, 1099, 1032, 833, 507	3.79 (s, 3 H), 4.37 (dd, J_1 = 6.9 Hz, J_2 = 2.3 Hz, 1 H), 5.13 (d, J = 2.3 Hz, 1 H), 6.47 (d, J = 6.9 Hz, 1 H), 6.83–6.94 (m, 4 H), 7.03 (d, J = 8.9 Hz, 2 H), 7.12 (d, J = 8.9 Hz, 2 H), 7.17–7.23 (m, 4 H), 7.69 (s, 1 H)	55.48, 63.64, 66.94, 114.88, 116.14 (d, J = 22.8 Hz), 119.48 (d, J = 8.0 Hz), 120.82, 127.59, 127.64, 128.30, 128.92, 133.23 (d, J = 2.8 Hz), 137.00, 155.07, 159.64 (d, J = 244.7 Hz), 160.45, 166.91	440.1152
4m	3321, 2935, 2836, 1742, 1649, 1610, 1552, 1506, 1386, 1303, 1292, 1223, 1174, 1136, 1030, 828	3.71 (s, 3 H), 3.78 (s, 3 H), 4.42 (dd, J_1 = 6.9 Hz, J_2 = 2.3 Hz, 1 H), 5.06 (d, J = 2.4 Hz, 1 H), 6.16 (s, 1 H), 6.70 (d, J = 8.9 Hz, 2 H), 6.81–6.92 (m, 4 H), 7.12 (d, J = 9.0 Hz, 2 H), 7.16–7.24 (m, 4 H, Ar-H), 7.28 (s, 1 H)	55.44, 55,56, 63.73, 67.09, 114.43, 114.77, 115.99 (d, J = 22.7 Hz), 119.34 (d, J = 7.9 Hz), 127.63, 128.05, 130.96, 133.50 (d, J = 2.4 Hz), 155.81, 159.45 (d, J = 244.3 Hz), 160.11, 166.36	436.1656

Compd.	FTIR-ATR ($\tilde{\nu}$/cm^{-1})	^{1}H NMR (600 MHz, $CDCl_3$) (δ/ppm)	^{13}C NMR (151 MHz, $CDCl_3$) (δ/ppm)	HRMS $(M+H)^+$
4n	3332, 2961, 1748, 1657, 1603, 1542, 1507, 1387, 1292, 1249, 1228, 1176, 1138, 1102, 1032, 831	1.25 (s, 9 H), 3.78 (s, 3 H), 4.46 (dd, J_1 = 6.8 Hz, J_2 = 2.3 Hz, 2 H), 5.06 (d, J = 2.3 Hz, 1 H), 6.18 (d, J = 6,8 Hz, 1 H), 6.84–6.90 (m, 4 H), 7.13–7.18 (m, 2 H), 7.18–7.23 (m, 6 H), 7.35 (s, 1 H)	31.49, 34.41, 55.45, 63.81, 67.07, 114.77, 116.00 (d, J = 22.8 Hz), 119.37 (d, J = 8.0 Hz), 120.99, 126.08, 127.66, 128.03, 133.49 (d, J = 2.6 Hz), 135.43, 147.06, 155.50, 159.47 (d, J = 244.5 Hz), 160.12, 166.22	462.2183
4o	3327, 2931, 1741, 1658, 1588, 1542, 1508, 1384, 1290, 1225, 1175, 1136, 1102, 1030, 830	2.20 (s, 3 H), 3.79 (s, 3 H), 4.39 (dd, J_1 = 6.9 Hz, J_2 = 2.3 Hz, 1 H), 5.12 (d, J = 2.3 Hz, 1 H), 6.48 (d, J = 6.9 Hz, 1 H), 6.82–6.85 (m, 6 H), 7.15–7.23 (m, 4 H), 7.27 (d, J = 2.0 Hz, 1 H), 7.62 (s, 1 H)	19.39, 55.46, 63.66, 66.94, 114.84, 116.10 (d, J = 22.7 Hz), 118,19, 119.48 (d, J = 7.9 Hz), 120.23, 127.62, 127.73, 130.65, 130.90, 133.25 (d, J = 2.6 Hz), 134.37, 137.17, 155.11, 159.59 (d, J = 244.7 Hz), 160.22, 160.41, 166.84	454.1257
4p	3320, 2918, 2851, 1753, 1645, 1612, 1566, 1508, 1387, 1279, 1247, 1224, 1175, 1153, 1102, 1031, 831	2.15 (s, 6 H), 3.78 (s, 3 H), 4.40 (dd, J_1 = 6.8 Hz, J_2 = 2.3 Hz, 1 H), 5.08 (d, J = 2.3 Hz, 1 H), 6.32 (d, J = 6.9 Hz, 1 H), 6.61 (s, 1 H), 6.75–6.94 (m, 6 H), 7.06–7.32 (m, 4 H), 7.40 (s, 1 H)	21.40, 55.43, 63.70, 67.03, 114.75, 116.01 (d, J = 22.8 Hz), 118.26, 119.38 (d, J = 8.0 Hz), 125.52, 127.64, 127.96, 133.43 (d, J = 2.7 Hz), 138.10, 138.78, 155.36, 159.45 (d, J = 244.2 Hz), 160.09, 166.58	434.1871
4r	3318, 1746, 1672, 1614, 1571, 1509, 1474, 1442, 1384, 1273, 1255, 1229, 1176, 1137, 1033, 836	3.81 (s, 3 H), 4.42 (dd, J_1 = 6.8 Hz, J_2 = 2.3 Hz, 1 H), 5.23 (d, J = 2.2 Hz, 1 H), 6.66 (d, J = 6.9 Hz, 1 H), 6.85–6.96 (m, 4H), 7.21–7.26 (m, 4 H), 7.31–7.35 (m, 1 H), 7.61–7.67 (m, 2 H), 8.20 (s, 1 H)	55.50, 63.74, 66.73, 115.01, 116.32 (d, J = 23.1 Hz), 118.26 (d, J = 4.1 Hz), 119.62 (d, J = 8.0 Hz), 120.43, 122.24, 124.05, 125.85, 127.15, 127.58, 132.07 (q, J = 33.3 Hz), 132.87 (d, J = 2.7 Hz), 140.02, 154.51, 159.89 (d, J = 245.8 Hz), 160.47, 167.10	542.1301
4s	3311, 2961, 1753, 1638, 1612, 1548, 1508, 1384, 1248, 1226, 1175, 1134, 1101, 1030, 831	2.29 (s, 6 H), 3.77 (s, 3 H), 4.44 (dd, J_1 = 6,8 Hz, J_2 = 2,3 Hz, 1 H), 4.96 (d, J = 2.3 Hz, 1 H), 6.39 (s, 1 H), 6.82–6.92 (m, 3 H), 7.03–7.16 (m, 3 H), 7.17–7.25 (m, 4 H)	18.48, 55.45, 63.91, 67.22, 114.75, 115.92 (d, J = 22.8 Hz), 119.09 (d, J = 7.8 Hz), 127.52, 128.23, 128.92, 133,70 (d, J = 2.6 Hz), 156.16, 159.33 (d, J = 243,7 Hz, C4, 4-FC_6H_4), 160.08, 166.04	434.1859
4t	3396, 3058, 2958, 1748, 1668, 1611, 1511, 1397, 1358, 1339, 1286, 1254, 1211, 1173, 1102, 1033, 834	3.77 (s, 3 H), 4.50 (dd, J_1 = 6.7 Hz, J_2 = 2.3 Hz, 1 H), 5.02 (d, J = 2.3 Hz, 1 H), 5,80 (s, 1 H), 6.79–6.90 (m, 4 H), 7.10 (s, 1 H), 7.16–7.24 (m, 4 H), 7.41 (t, J = 7.8 Hz, 1 H), 7.47–7.54 (m, 2 H), 7.61 (d, J = 7.4 Hz, 1 H), 7.72 (d, J = 8.2 Hz, 1 H), 7.82–7.89 (m, 1 H), 7.99–8.09 (m, 1 H)	55.47, 63.80, 67.23, 114.78, 115.97 (d, J = 22.8 Hz), 119.19 (d, J = 7.9 Hz), 122.03, 123.96, 125.97, 126.85, 127.20, 127.61, 127.69, 128.15, 128.75, 129.61, 132.46, 133.67 (d, J = 2.6 Hz), 134.70, 156.00, 159.40 (d, J = 243.9 Hz), 160.14, 164.76	456.1714

[a] Compound **1** was ascertained by elemental analysis; calcd. C 73.35, H 5.28, N 6.11; found C 73.06, H 5.40, N 6.12

Antimicrobial activity

All newly synthesised *β*-lactams derivatives were subsequently tested for their antibacterial and antifungal activities (data not shown). The results showed that compounds **4a–t** did not inhibit the growth of three indicator bacterial species and two fungal species in the tested range of 128–0.125 μg mL^{-1}. It is well known that the 2-azetidinone ring is the pharmacophore responsible for the antibacterial and antifungal activity of many structurally diverse compounds (12). It is surprising that the tested compounds did not exhibit antibacterial or antifungal activity. A possible explanation for the experimental results could be found in the substitution at the *β*-lactam ring. All synthesized *β*-lactam ureas **4a–t** contain a 4-fluorophenyl group at the N1 position of the *β*-lactam and a 4-methoxyphenyl group at the C4 position of the *β*-lactam as well as an alkyl-, aryl-, cycloalkyl- or heterocycle-substituted N-atom of the ureido group attached to the C3 position of the *β*-lactam ring. The results show that these substituents have no significant effect on the antimicrobial activity.

Antiproliferative activity

The synthesized compounds **4a**, **4b**, **4c**, **4f**, **4h**, **4n**, **4o**, **4p**, and **4s** were tested *in vitro* for their antiproliferative activity against a panel of three human cancer cell lines HepG2 (liver), A2780 (ovarian), MCF7 (breast), and a healthy cell line HFF1 (human fibroblasts). The results are summarized in Table III. All of the tested compounds show antiproliferative activity against at least two of the three tested cancer cell lines with IC_{50} values within the range 7.8 ± 8.4 to 82 ± 85 μmol L^{-1}. Compound with 3-chloro-4-methylphenyl substituent (**4o**), showed the most potent antiproliferative profile against studied cancer cell lines, with the lowest IC_{50} value of 7.8 ± 8.4 μmol L^{-1} on ovarian carcinoma cell line A2870. However, this *β*-lactam urea as well as the majority of other tested molecules, is also toxic to normal human skin fibroblasts as well as HFF1 (Table III). The majority of tested compounds were cytotoxic to HFF1 cells. In particular, compounds **4o** and **4p** exerted the strongest antiproliferative effect on HFF1, while *β*-lactam ureas **4f**, **4n** were less toxic to healthy HFF1 cells compared to the cancer cell lines. Compounds **4a** and **4s** did not show antiproliferative effect on HFF1 nor on HepG2 cells. Taken together, it appears that no selectivity is achieved for compounds **4o** and **4p**, as they showed toxicity to all cell lines tested. On the other hand, compounds **4a** and **4s** showed clear antiproliferative activity against the A2780 and MCF7 cell lines, but no activity against the HepG2 and HFF1 cell lines (> 100 μmol L^{-1}). It is important to note that the substitution at the urea moiety proved to be crucial for toxicity and antiproliferative activity, which is not the case for antimicrobial activity. The highest toxicity for all tested cell lines is obtained with the 3,5-dimethylphenyl (**4p**) and 3-chloro--4-methylphenyl (**4o**) substitution at the urea moiety. In contrast, allyl (**4a**) and 2,6-dimethylphenyl (**4s**) substituents have been shown to be the least toxic; surprisingly, only a slight difference in the position of the methyl group in compounds **4p**/**4s** showed a major impact on bioactivity.

In silico *physicochemical and biological profiling*

Herein, ADMET properties for the synthesised compounds **4a–t** were estimated by the program ADMET Predictor 9.5 (43) and the web server admetSAR (44).

Table III. In vitro *antiproliferative activity of compounds* ***4a***, ***4b***, ***4c***, ***4f***, ***4h***, ***4n***, ***4o***, ***4p***, *and* ***4s*** *against the HepG2, A2780, MCF7 and HFF1 cell lines determined by MTT assay*

Compd.	IC_{50} (μmol L^{-1})[a]			
	HepG2	A2780	MCF7	HFF1
4a	>100	25.1 ± 4.0	57.0 ± 22.1	>100
4b	18.0 ± 0.1	16.2 ± 0.3	17.7 ± 0.5	18.3 ± 0.1
4c	17.9 ± 1.3	16.4 ± 0	20.0 ± 3.7	17.0 ± 0.7
4f	82.4 ± 85.1	20.1 ± 3.8	19.3 ± 1.7	64.2 ± 16.0
4h	17.1 ± 1.5	11.8 ± 0.2	14.9 ± 6.1	19.1 ± 1.0
4n	30.0 ± 48.0	13.0 ± 5.2	12.3 ± 1.7	48.4 ± 26.1
4o	17.4 ± 5.3	7.8 ± 8.4	13.0 ± 2.2	8.0 ± 5.1
4p	23.9 ± 0.8	16.3 ± 0.2	18.2 ± 0.1	4.5 ± 8.9
4s	>100	23.1 ± 1.9	43.2 ± 13.1	>100

Human cancer cell lines: HepG2 (liver), A2780 (ovarian) and MCF7 (breast). Normal cell line: HFF1 (human fibroblast).

[a] IC_{50} (concentration that causes 50 % growth inhibition) ± SD (each test was performed in quadruplicate in two individual experiments).

All synthesised *β*-lactam ureas, with the exception of **4r**, conform to Lipinski's and Veber's rules for drug-like, low molecular mass compounds (Table SI). An orally administered molecule as per Lipinski's rule of five should have log*P* ≤ 5, M_r < 500 Da, HBD ≤ 5, and HBA ≤ 10 (49–51), while according to Veber's rule (52) its TPSA and the number of rotatable bonds should be less than 140 $Å^2$ (or 12 or fewer HBD and HBA) and 10, resp. The outlier **4r** with 3,5-bis(trifluoromethyl) substituent violates Lipinski's rule in terms of molecular mass (M_r = 541.43) and lipophilicity (log*P* = 5.46). As it is well known, lipophilicity being a very important property of a drug strongly affects its pharmacokinetics, pharmacodynamics, and toxicological profile, *i.e.*, solubility, absorption, distribution, metabolism, excretion, binding to plasma proteins, interaction with the receptor, transport across cell membranes and BBB (53). All *β*-lactam ureas **4a–t** are estimated to be non-ionisable compounds with log*P* lying within the range 2.5–5.0 (except **4r**). They are predicted to have moderate water solubility which agrees with our observation (Table SI), and moderate to high membrane permeability (Table SII), which altogether indicates their good oral bioavailability.

Good membrane permeability of a compound may be affected by its interaction with efflux pumps such as P-glycoprotein (Pgp). According to ADMET predictor models, all synthesised *trans-β*-lactam ureas **4a–t** are estimated to be Pgp substrates, and many of them are predicted to be Pgp inhibitors (Table SII). The BBB is a selectively permeable membrane that controls the passage of molecules into and out of the brain (54). Considering that *β*-lactam ureas **4a–t** are predicted to be Pgp substrates, not penetrate BBB, and have low retention in the brain (BBB and logBB parameters in Table SII, resp.), it is likely that they do not enter the brain. As for the distribution in the body, the synthesised molecules are likely to be transported through the body by plasma proteins (low hum_fup% values in Table SII).

With regard to metabolism, the web server admetSAR was used to estimate the likelihood that the compounds are substrates and inhibitors of cytochrome P450 (CYP450) enzymes. These oxidoreductases belong to a superfamily of heme-containing proteins involved in the phase I metabolism of drugs and other xenobiotics (55, 56). Among CYP450 enzymes, the CYP1, CYP2, and CYP3 families mediate 70–80 % of all phase I metabolic reactions of clinically relevant drugs with CYP3A4 performing at least half of the drug metabolism (57, 58). According to admetSAR predictions, all *trans*-β-lactam ureas **4a–t** should be substrates for CYP3A4 (and not for other considered CYPs), and half of them are also predicted to be its inhibitors (Table SII). This also implies the importance of determining cellular metabolites when interpreting *in vitro* results. The CYP450-mediated intrinsic clearance of β-lactam ureas is also supported by quite low estimated fractions of unbound compounds in human liver microsomes (%Fumic). These compounds are classified as class 2 of the extended clearance classification system (ECCS), with hepatic metabolism being the major route of excretion. Class 2 molecules (high permeability bases/neutral substances) (59) tend to be predominantly metabolized in the liver by enzymes such as CYP3A4. They cross the basolateral membrane of hepatocytes by passive diffusion and are metabolised and excreted in the urine/bile as phase I or II metabolites (60).

The synthetized compounds should have low hepatotoxicity and mutagenicity. The β-lactam ureas **4r** and **4t** were predicted as the most potentially toxic molecules with potentially having negative cardiotoxic and carcinogenic impacts (Table SII).

The PASS software (45) and SwissTargetPrediction online server (46) were used to envision the biological activities of nineteen *trans*-β-lactam ureas **4a–t**. By using built-in machine-learning models, PASS simultaneously predicts more than a thousand biological and toxicological activities from the 2D structural formulae of the compounds. On the other hand, SwissTargetPrediction estimates likely protein targets based on structural similarity with 327,719 already known actives on 2,092 human proteins. Although PASS predicted 177 possible activities for at least one of the new β-lactams including treatment of atherosclerosis, and anti-inflammatory and analgesic activity which are consistent with the already known activities of this chemical class, they were predicted with Pa $\leq$ 0.5 (Table SIII). Similarly, according to SwissTargetPrediction a list of human proteins, mainly kinases, were suggested as tentative targets with low probability. No predictions were found by either algorithm with high probability as there were no similar chemicals in the training models of PASS and among the SwissTargetPrediction active compounds, indicating a substantial novelty in the structures of the synthesized β-lactam ureas.

Limitations of the study

In this research, compounds involved in synthesis and evaluation aimed to yield new products that possess interesting biological activities. All these compounds have a common chemical β-lactam moiety, which usually has a broad spectrum of activities, especially the antimicrobial activity, which is completely absent in our study. In contrast to this finding, their biological profile included antiproliferative activities. More detailed prospects for future studies on this class of bioactive compounds are expected and will also be extended after the chemical conversion of β-lactam ureas into hydantoin derivatives, possibly as a continuation paper.

CONCLUSIONS

In conclusion, a series of nineteen novel drug-like racemic β-lactam ureas **4a–t** were synthesised in good to excellent yields. Their biological potential was evaluated *in vitro* by testing the antimicrobial and antiproliferative activities and *in silico* by using PASS, SwissTargetPrediction, and ADMET predictor approaches. Neither of the β-lactam ureas racemates showed antibacterial activity against *E. coli*, *P. aeruginosa*, and *S. aureus* and antifungal activity against *C. albicans* and *S. cerevisiae*. Most of the tested compounds **4a**, **4b**, **4c**, **4f**, **4h**, **4n**, **4o**, **4p**, and **4s** showed antiproliferative activity on tested tumor cell lines HepG2, A2780, and MCF-7 in the micromolar range, but were also cytotoxic for normal fibroblasts HFF-1. The β-lactam urea **4o** with 3-chloro-4-methylphenyl substituent (IC_{50} = 7.8 ± 8.4 μmol L^{-1}) was found to have promising antitumor activity against ovarian carcinoma cell A2780; however, compounds **4o** and **4p** showed a strong cytotoxic effect against normal cell line HFF (IC_{50} = 8.0 ± 5.1 μmol L^{-1} and IC_{50} = 4.5 ± 8.9 μmol L^{-1}, resp.). In addition, compounds **4a**, **4f**, **4n**, and **4s** exerted no or low toxic effects on human fibroblasts HFF-1 in the studied concentration range. *In silico* ADMET profiling described compounds **4a–t** as moderately water-soluble and membrane permeable, quite lipophilic molecules with a propensity to be metabolised by CYP3A4 (and excreted hepatically) and expelled by Pgp pump. PASS and SwissTargetPrediction predicted some significant biological activities and targets for compounds **4a–t** but with low probability, consistent with the novelty of their structure. Considering predicted activities, *e.g.*, atherosclerosis treatment, and low toxicity risk on human fibroblasts, molecules **4a** and **4f** can be suggested as the most promising for further investigations comprising chemical structure modifications.

Supplementary materials are available upon request.

Acknowledgments. – We would like to thank the NMR Centre for recording the spectra.

Funding. – This study was supported by the Croatian Government and the European Union through the European Regional Development Fund – the Competitiveness and Cohesion Operational Programme (KK.01.1.1.01) through the project Bioprospecting of the Adriatic Sea (KK.01.1.1.01.0002) granted to The Scientific Centre of Excellence for Marine Bioprospecting – BioProCro.

Conflicts of interest. – The authors declare no conflict of interest.

Authors contributions. – Conceptualization, M.J., T.D. and M.R.; methodology, M.J., V.S., K.B. and D.V.; analysis, M.J., K.B. and D.V.; investigation, M.J., V.S., K.B. and D.V.; writing, original draft preparation, M.J., V.S. and K.B.; writing, review, and editing, D.K., T.D. and M.R. All authors have read and agreed to the published version of the manuscript.

REFERENCES

1. A. R. Deshmukh, B. M. Bhawal, D. Krishnaswamy, V. V. Govande, B. A. Shinkre and A. Jayanthi, Azetidin-2-ones, synthon for biologically important compounds, *Curr. Med. Chem.* **11**(14) (2004) 1889–1920; https://doi.org/10.2174/0929867043364874
2. M. Bortolami, I. Chiarotto, L. Mattiello, R. Petrucci, D. Rocco, F. Vetica and M. Feroci, Organic electrochemistry: Synthesis and functionalization of β-lactams in the twenty-first century, *Heterocycl. Commun.* **27**(1) (2021) 32–44; https://doi.org/10.1515/hc-2020-0121
3. K. Poole, Resistance to β-lactam antibiotics, *Cell. Mol. Life Sci.* **61** (2004) 2200–2223; https://doi.org/10.1007/s00018-004-4060-9

4. S. Y. Essack, The development of β-lactam antibiotics in response to the evolution of β-lactamases, *Pharm. Res.* **18** (2001) 1391–1399; https://doi.org/10.1023/A:1012272403776
5. D. M. Livermore and J. D. Williams, *β-lactams: Mode of Action and Mechanisms of Bacterial Resistance*, in *Antibiotics in Laboratory Medicine* (Ed. V. Lorian), 4th ed., Williams and Wilkins, Baltimore 1996, pp. 502–577.
6. C. Palomo, J. M. Aizpurua, I. Ganboa and M. Oiarbide, β-lactams as versatile intermediates in α- and β-amino acid synthesis, *Synlett.* **12** (2001) 1813–1826; https://doi.org/10.1055/s-2001-18733
7. B. Alcaide, P. Almendros and C. Aragoncillo, β-lactams: versatile building blocks for the stereoselective synthesis of non-β-lactam products, *Chem. Rev.* **107**(11) (2007) 4437–4492; https://doi.org/10.1021/cr0307300
8. A. K. Halve, D. Bhadauria and R. Dubey, N/C-4 substituted azetidin-2-ones: synthesis and preliminary evaluation as new class of antimicrobial agents, *Bioorg. Med. Chem. Lett.* **17**(2) (2007) 341–345; https://doi.org/10.1016/j.bmcl.2006.10.064
9. B. Hamad, The antibiotics market, *Nat. Rev. Drug Discov.* **9** (2010) 675–676; https://doi.org/10.1038/nrd3267
10. S. Zavar, M. Zarei and M. Saraei, Synthesis of β-lactams via Staudinger reaction using N-ethoxycarbonyl-2-ethoxy-1,2-dihydroquinoline as a carboxylic acid activator, *Synth. Commun.* **46**(24) (2016) 2031–2036; https://doi.org/10.1080/00397911.2016.1244691
11. A. Kamath and I. Ojima, Advances in the chemistry of β-lactam and its medicinal applications, *Tetrahedron* **68**(52) (2012) 10640–10664; https://doi.org/10.1016/j.tet.2012.07.090
12. P. D. Mehta, N. P. S. Sengar and A. K. Pathak, 2-Azetidinone – a new profile of various pharmacological activities, *Eur. J. Med. Chem.* **45**(12) (2010) 5541–5560; https://doi.org/10.1016/j.ejmech.2010.09.035
13. A. Jarrahpour, P. Shirvani, V. Sinou, C. Latour and J. M. Brunel, Synthesis and biological evaluation of some new β-lactam-triazole hybrids, *Med. Chem. Res.* **25** (2016) 149–162; https://doi.org/10.1007/s00044-015-1474-x
14. A. Jarrahpour, P. Shirvani, V. Sinou, C. Latour and J. M. Brunel, Diastereoselective synthesis of potent antimalarial *cis*-β-lactam agents through a [2+2] cycloaddition of chiral imines with a chiral ketene, *Eur. J. Med. Chem.* **87** (2014) 364–371; http://dx.doi.org/10.1016/j.ejmech.2014.09.077
15. D. A. Burnett, β-lactam cholesterol absorption inhibitors. β-lactam cholesterol absorption inhibitors, *Curr. Med. Chem.* **11**(14) (2004) 1873–1887; https://doi.org/10.2174/0929867043364865
16. J. C. Sutton, S. A. Bolton, K. S. Hartl, M.-H. Huang, G. Jacobs, W. Meng, M. Ogletree, Z. Pi, W. A. Schumacher, S. M. Seiler, W. A. Slusarchyk, U. Treuner, R. Zahler, G. Zhao and G. S. Bisacchi, Synthesis and SAR of 4-carboxy-2-azetidinone mechanism-based tryptase inhibitors, *Bioorg. Med. Chem. Lett.* **12**(21) (2002) 3229–3233; https://doi.org/10.1016/S0960-894X(02)00688-1
17. A. D. Borthwick, G. Weingarten, T. M. Haley, M. Tomaszewski, W. Wang, Z. Hu, J. Bedard, H. Jin, L. Yuen and T. S. Mansour, Design and synthesis of monocyclic β-lactams as mechanism-based inhibitors of human cytomegalovirus protease, *Bioorg. Med. Chem. Lett.* **8**(4) (2008) 365–370; https://doi.org/10.1016/s0960-894x(98)00032-8
18. C. D. Guillon, G. A. Koppel, M. J. Brownstein, M. O. Chaney, C. F. Ferris, S.-f. Lu, K. M. Fabio, M. J. Miller, N. D. Heindel, D. C. Hunden, R. D. G. Cooper, S. W. Kaldor, J. J. Skelton, B. A. Dressman, M. P. Clay, M. I. Steinberg, R. F. Bruns and N. G. Simon, Azetidinones as vasopressin V1a antagonists, *Bioorg. Med. Chem.* **15**(5) (2007) 2054–2080; https://doi.org/10.1016/j.bmc.2006.12.031
19. N. M. O'Boyle, M. Carr, L. M. Greene, O. Bergin, S. M. Nathwani, T. McCabe, D. G. Lloyd, D. M. Zisterer and M. J. Meegan, Synthesis and evaluation of azetidinone analogues of combretastatin A-4 as tubulin targeting agents, *J. Med. Chem.* **53**(24) (2010) 8569–8584; https://doi.org/10.1021/jm101115u

20. B. K. Banik, I. Banik and F. F. Becker, Asymmetric synthesis of anticancer β-lactams via Staudinger reaction: utilization of chiral ketene from carbohydrate, *Eur. J. Med. Chem.* **45**(2) (2010) 846–848; https://doi.org/10.1016/j.ejmech.2009.11.024
21. R. Sharma, P. Samadhiya, S. D. Srivastava and S. K. Srivastava, Synthesis and biological activity of new series of *N*-[3-(1H-1,2,3- benzotriazol-1-yl)propyl]-2-(substituted phenyl)-3-chloro-4-oxo-1-azetidinecarboxamide, *Acta Chim. Slov.* **58**(1) (2011) 110–119.
22. T. Sperka, J. Pitlik, P. Bagossi and J. Tözsér, Beta-lactam compounds as apparently uncompetitive inhibitors of HIV-1 protease, *Bioorg. Med. Chem. Lett.* **15**(12) (2005) 3086–3090; https://doi.org/10.1016/j.bmcl.2005.04.020
23. C. Saturnino, B. Fusco, P. Saturnino, G. D. E. Martino, F. Rocco and J.-C. Lancelot, Evaluation of analgesic and anti-inflammatory activity of novel beta-lactam monocyclic compounds, *Biol. Pharm. Bull*. **23**(5) (2000) 654–656; https://doi.org/10.1248/bpb.23.654
24. R. K. Goel, M. P. Mahajan and S. K. Kulkarni, Evaluation of anti-hyperglycemic activity of some novel monocyclic β-lactams, *J. Pharm. Pharm. Sci.* **7**(1) (2004) 80–83.
25. A. Jarrahpour, E. Ebrahimi, R. Khalifeh, H. Sharghi, M. Sahraei, V. Sinou, C. Latour and J. M. Brunel, Synthesis of novel β-lactams bearing an anthraquinone moiety, and evaluation of their antimalarial activities, *Tetrahedron* **68**(24) (2012) 4740–4744; https://doi.org/10.1016/j.tet.2012.04.011
26. S. Hosseyni and A. Jarrahpour, Recent advances in β-lactam synthesis, *Org. Biomol. Chem.* **16** (2018) 6840–6852; https://doi.org/10.1039/C8OB01833B
27. C. R. Pitts and T. Lectka, Chemical synthesis of β-lactams: Asymmetric catalysis and other recent advances, *Chem. Rev.* **114**(16) (2014) 7930–7953; https://doi.org/10.1021/cr4005549
28. S. Deketelaere, T. Van Nguyen, C. V. Stevens and M. D'hooghe, Synthetic approaches toward monocyclic 3-amino-β-lactams, *ChemistryOpen* **6**(3) (2017) 301–319; https://doi.org/10.1002/open.201700051
29. N. Payili, S. Yennam, S. R. Rekula, C. G. Naidu, Y. Bobde and B. Ghoshc, Design, synthesis, and evaluation of the anticancer properties of novel quinone bearing carbamyl β-lactam hybrids, *J. Heterocyclic Chem.* **55**(6) (2018) 1358–1365; https://doi.org/10.1002/jhet.3169
30. L. Jiao, Y. Liang and J. Xu, Origin of the relative stereoselectivity of the β-lactam formation in the Staudinger reaction, *J. Am. Chem. Soc.* **128**(18) (2006) 6060–6069; https://doi.org/10.1021/ja056711k
31. F. P. Cossío, A. de Cózar, S. M. Sierra, L. Casarrubios, J. G. Muntaner, B. K. Banik and D. Bandyopadhyay, Role of imine isomerization in the stereocontrol of the Staudinger reaction between ketenes and imines, *RSC Adv.* **12** (2021) 104–117; https://doi.org/10.1039/d1ra06114c
32. T. C. Malig, D. Yu and J. E. Hein, A revised mechanism for the Kinugasa reaction, *J. Am. Chem. Soc.* **140**(29) (2018) 9167–9173; https://doi.org/10.1021/jacs.8b04635
33. F. Toda, H. Miyamoto, M. Inoue, S. Yasaka and I. Matijasic, Enantioselective photocyclization of amides to beta-lactam derivatives in inclusion crystals with an optically active host, *J. Org. Chem.* **65**(9) (2000) 2728–2732; https://doi.org/10.1021/jo991832m
34. Z. Wang, J. Ni, Y. Kuninobu and M. Kanai, Copper-catalyzed intramolecular C(sp^3)H and C(sp^2)H amidation by oxidative cyclization, *Angew. Chem. Int. Ed.* **53**(13) (2014) 3496–3499; https://doi.org/10.1002/anie.201311105
35. S. France, A. Weatherwax, A. E. Taggi and T. Lectka, Advances in the catalytic, asymmetric synthesis of β-lactams, *Acc. Chem. Res.* **37**(8) (2004) 592–600; https://doi.org/10.1021/ar030055g
36. T. Dražić, M. Roje, M. Jurin and G. Pescitelli, Synthesis, separation and absolute configuration determination by ECD Spectroscopy and TDDFT calculations of 3-amino-β-lactams and derived guanidines, *Eur. J. Org. Chem.* **2016**(24) (2016) 4189–4199; https://doi.org/10.1002/ejoc.201600641
37. Clinical and Laboratory Standards Institute, *Methods for Dilution Antimicrobial Susceptibility Tests for Bacteria That Grow Aerobically*, 11th ed., CLSI standard M07, CLSI, Wayne (PA, USA) 2018; https://clsi.org/media/1928/m07ed11_sample.pdf; last access date April 6, 2020

38. J. M. Andrews, Determination of minimum inhibitory concentrations, *J. Antimicrob. Chemother.* **48**(Suppl. S1) (2001) 5–16; https://doi.org/10.1093/JAC/48.SUPPL_1.5

39. Clinical and Laboratory Standards Institute, *Reference Method for Broth Dilution Antifungal Susceptibility Testing of Filamentous Fungi*, 3rd ed., CLSI standard M38, CLSI, Wayne (PA, USA) 2017; https://clsi.org/media/1894/m38ed3_sample.pdf; last access date April 27, 2020

40. M. Hranjec, M. Kralj, I. Piantanida, M. Sedić, L. Šuman, K. Pavelić and G. Karminski-Zamola, Novel cyano- and amidino-substituted derivatives of styryl-2-benzimidazoles and benzimidazo[1,2-a]quinolines. synthesis, photochemical synthesis, DNA binding and antitumor evaluation, Part 3, *J. Med. Chem.* **50**(23) (2007) 5696–5711; https://doi.org/10.1021/jm070876h

41. M. Hranjec, I. Piantanida, M. Kralj, L. Šuman, K. Pavelić and G. Karminski-Zamola, Novel amidino-substituted thienyl- and furylvinyl-benzimidazole derivatives and their photochemical conversion into corresponding diaza-cyclopenta[c]fluorenes. Synthesis, interactions with DNA and RNA and antitumor evaluation, *J. Med. Chem.* **51**(16) (2008) 4899–4910; https://doi.org/10.1021/jm8000423

42. M. R. Boyd and K. D. Paull, Some practical considerations and applications of the national cancer institute *in vitro* anticancer drug discovery screen, *Drug Dev. Res.* **34**(2) (1995) 91–109; https://doi.org/10.1002/ddr.430340203

43. M. S. Lowless, M. Waldman, R. Franczkiewicz and R. D. Clark, *Using Chemoinformatics in Drug Discovery*, in *New Approaches to Drug Discovery, Handbook of Experimental Pharmacology* (Eds. U. Nielsch, U. Fuhrmann and S. Jaroch), Vol. 232, Springer Int. Publ. Switzerland, Cham 2016, pp. 232, 139–170.

44. H. Yang, C. Lou, L. Sun, J. Li, Y. Cai, Z. Wang, W. Li, G. Liu and Y. Tang, admetSAR 2.0: web-service for prediction and optimization of chemical ADMET properties, *Bioinformatics* **35**(6) (2019) 1067–1069; https://doi.org/10.1093/bioinformatics/bty707

45. D. A. Filimonov and V. V. Poroikov, *Probabilistic Approach in Activity Prediction*, in *Chemoinformatics Approaches to Virtual Screening* (Eds. A. Varnek and A. Tropsha), RSC Publishing, Cambridge (UK) 2008, pp. 182–216.

46. A. Daina, O. Michielin and V. Zoete, SwissTargetPrediction: updated data and new features for efficient prediction of protein targets of small molecules, *Nucleic Acids Res.* **47**(W1) (2019) W357–W364; https://doi.org/10.1093/nar/gkz382

47. D. Bandyopadhyay, J. Cruz and B. K. Banik, Novel synthesis of 3-pyrrole substituted β-lactams via microwave-induced bismuth nitrate-catalyzed reaction, *Tetrahedron* **68**(52) (2012) 10686–10695; https://doi.org/10.1016/j.tet.2012.06.009

48. K. Radolović, I. Habuš and B. Kralj, New thiazolidinone and triazinethione conjugates derived from amino-β-lactams, *Heterocycles* **78**(7) (2009) 1729–1759; https://doi.org/10.3987/COM-09-11668

49. C. A. Lipinski, F. Lombardo, B. W. Dominy and P. J. Feeney, Experimental and computational approaches to estimate solubility and permeability in drug discovery and development settings, *Adv. Drug Deliv. Rev.* **23**(1–3) (1997) 3–25; https//doi.org/10.1016/S0169-409X(96)00423-1

50. C. A. Lipinski, F. Lombardo, B. W. Dominy and P. J. Feeney, Experimental and computational approaches to estimate solubility and permeability in drug discovery and development settings, *Adv. Drug Deliv. Rev.* **64**(Suppl.) (2012) 4–17; https://doi.org/10.1016/j.addr.2012.09.019

51. C. A. Lipinski, Drug-like properties and the causes of poor solubility and poor permeability, *J. Pharmacol. Toxicol. Method* **44**(1) (2000) 235–249; https//doi.org/10.1016/s1056-8719(00)00107-6

52. D. F. Veber, S. R. Johnson, H. Y. Cheng, B. R. Smith, K. W. Ward and K. D. Kopple, Molecular properties that influence the oral bioavailability of drug candidates, *J. Med. Chem.* **45**(12) (2002) 2615–2623; https://doi.org/10.1021/jm020017n

53. S. Lobo, Is there enough focus on lipophilicity in drug discovery?, *Expert Opin. Drug Discov.* **15**(3) (2019) 261–263; https://doi.org/10.1080/17460441.2020.1691995

54. R. Haddad-Tóvolli, N. R. V. Dragano, A. F. S. Ramalho and L. A. Velloso, Development and function of the blood-brain barrier in the context of metabolic control, *Front. Neurosci.* **11** (2017) Article ID 224 (12 pages); https://www.frontiersin.org/articles/10.3389/fnins.2017.00224

55. E. Stavropoulou, G. G. Pircalabioru and E. Bezirtzoglou, The role of cytochromes P450 in infection, *Front. Immunol.* **9** (2018) Article ID 89 (7 pages); https://doi.org/10.3389/fimmu.2018.00089

56. A. M. McDonnell and C. H. Dang, Basic review of the cytochrome p450 system, *J. Adv. Pract. Oncol.* **4** (2013) 263–268; https://doi.org/10.6004/jadpro.2013.4.4.7

57. F. P. Guengerich, Cytochrome P450 and chemical toxicology, *Chem. Res. Toxicol.* **21**(1) (2008) 70–83; https://doi.org/10.1021/tx700079z

58. B. Testa, A. Pedretti and G. Vistoli, Reactions and enzymes in the metabolism of drugs and other xenobiotics, *Drug Discov. Today* **17**(11–12) (2012) 549–560; https://doi.org/10.1016/j.drudis.2012.01.017

59. A. F. El-Kattan and M. V. S. Varma, Navigating transporter sciences in pharmacokinetics characterization using the extended clearance classification system, *Drug. Metab. Dispos.* **46**(5) (2018) 729–739; https://doi.org/10.1124/dmd.117.080044

60. M. V. Varma, S. J. Steyn, C. Allerton and A. F. El-Kattan, Predicting clearance mechanism in drug discovery: Extended clearance classification system (ECCS), *Pharm. Res.* **32** (2015) 3785–3802; https://doi.org/10.1007/s11095-015-1749-4